Low Velocity Impact on Relatively Thick Rectangular Plate under In-plane Loads Resting on Pasternak Elastic Foundation

Sh. Hosseini Hashemi[*]
Associate Professor

R. Kalhor[†]
M. Sc Student

This study deals with the elastic-plastic impact on moderately thick rectangular plate subjected to uniform in-plane compressive loads resting on the Pasternak elastic foundation. The proposed rectangular plates have two opposite edges simply-supported, while all possible combinations of free, simply-supported and clamped boundary conditions are applied to the other two edges. The dimensionless equations of motion of the plate are obtained by applying the Reissner-Mindlin plate theory considering the first-order shear deformation and the rotary inertia effects. The exact closed form solution of the governing equations leading to more accurate result with less calculating time in comparison with the Rayleigh-Ritz method is used to obtain the dynamic response of the plat. The validity of the result is first examined by studying the convergence of the maximum impact force. Then, a comparison of results with those available in literature confirms the excellent accuracy of the present approach. Finally the effects of the dimensionless parameters such as uniaxial and biaxial in-plane loads and the effect of foundation stiffness parameters on force and displacement histories have been examined.

Keywords: Low velocity impact, first order shear deformation theory, permanent indentation, in-plane loads, elastic foundation

1 Introduction

Rectangular plates, subjected to external in-plane loads, with different sizes, thickness variations and boundary conditions have undoubtedly been one of the key components in aerospace, civil, automotive, optical, electronic, mechanical, and shipbuilding industries. They may also be supported by an elastic foundation. These kinds of plates are mainly used in concrete roads, raft, and mat foundations of buildings and reinforced concrete pavements of airport runways. Abrate [1] implied that the first step for thorough understanding of impact event is choosing an appropriate model for prognosis force and displacement histories that involves the motion of the target, the motion of the projectile, and the local indentation in the contact zone. Hence many models have been proposed in the literature. These models can be classified into three categories: (1) energy-balance models that assume a quasi-static behavior of the structure; (2) spring-mass models that account for the dynamics of the structure in a

---

[*]Corresponding Author, Associate Professor, Impact Research Laboratory, School of Mechanical Engineering, Iran University of Science and Technology, Narmak, Tehran 16846-13114, Iran
shh@iust.ac.ir
[†] M. Sc Student, Impact Research Laboratory, School of Mechanical Engineering, Iran University of Science and Technology, Narmak, Tehran 16846-13114, Iran

simplified manner; (3) complete models in which the dynamic behavior of the structure is fully modeled. First step for complete modeling of low velocity impact on rectangular plate under in-plane load resting on elastic foundation is forced vibration solution of it. Lee and Reismann [2] investigated forced vibration of a rectangular plate with simply supported boundary condition under transverse impact loading with 3-D elasticity theory. Reismann and Tendorf [3] solved forced vibration of thick isotropic plates by using modal superposition approach. In another study Reismann and Lxu [4] surveyed forced vibration of rectangular plate with simply supported boundary condition under initial stresses and time independent mechanical transverse load by applying 3-D elasticity solution. Sakata and Sakata [5] studied forced vibration of rectangular plate with varying thickness and SFSF boundary conditions under mechanical transverse load accompanied by sinusoidal displacement distribution, constant, and harmonic time functions by utilizing approximate functions for forced vibration. Laura [6] analyzed forced vibration of non-isotropic rectangular plates with simply supported boundary condition by using Rayleigh-Ritz method. Shen [7] and Yu [8] studied free and forced vibration of relatively thick plates by applying the Reissner-Mindlin plate theory with totally free boundary conditions. In another paper, Shen [9] analyzed free and force vibration of relatively Reissner-Mindlin rectangular plate with simply supported boundary conditions exposed to thermomechanical loading and resting on a Pasternak-type elastic foundation. The mechanical loads consisted of transverse partially distributed impulsive loads and in-plane edge loads while the temperature field is assumed to exhibit a linear variation through the thickness of the plate. The Modal Superposition Approach and State Variable Approach are both used to determine the dynamic response of the plate.

Rossikhin and Shitikova [10] considered the problem of normal impact of a long thin elastic cylindrical rod upon an infinite pre-stressed elastic transversely isotropic plate possessing cylindrical anisotropy. The impact took place at the center of the plate, whose equations of motion considered both rotary inertia and shear deformations. It was shown that as the radial compression forces reach a critical magnitude, the velocity and amplitude of the transient wave of transverse shear both diminish to zero. Sun and Chattopadhyay [11] investigated the dynamic response to the impact of a mass on rectangular anisotropic laminated plates under an initial tensile stress. The equations of plate motion took the transverse shear deformations into account, but ignored the rotary inertia in the direction of coordinate axes lying in the plate's median plane. As a result, the Timoshenko nonlinear integral equation for the contact force was used, which was then solved numerically by means of the small-time increment method. It is shown that, a higher initial tensile stress elevates the maximum contact force, but reduces the contact time, the deflection, and the stresses, as well as increases the velocity of disturbance propagation. Dynamic response of pre-stressed composite laminates subjected to large deflection impact is investigated by Sun and Chen [12] using the finite element method. They found that an initial tensile stress tends to intensify the contact force while reducing the contact time. It was also noted that an initial compressive stress may result in larger amplitudes of deflection.

Wei and Yida [13] considered the dynamic response of an elastic plate with arbitrary boundary shape supported by a linear viscoelastic Winkler foundation, and impacted by a low velocity projectile. Classical plate theory was used in this article. Nath and Varma [14] studied nonlinear dynamic response of clamped and simply supported plates resting on Winkler-Pasternak elastic foundation subjected to the uniform step and sinusoidal loadings. The effects of Winkler and shear foundation interaction parameters on the response of the plates have been investigated.

Shear deformation effects on impact force and displacement histories are broadly investigated through references [15-18] and importance of using first order shear deformation theory were

emphasized. In these studies, frequencies and mode shapes were acquired by using power series and Rayleigh-Ritz methods. Leissa and Kang [19-21] have also obtained exact solutions for free vibration and buckling of a thin rectangular plate by using power series method. Hosseini-Hashemi and et al. [22] have presented the exact solution for free vibration of moderately thick rectangular plate. They obtained exact characteristic equations for six distinct cases involving all possible combinations of classical boundary conditions namely SSSS, SCSS, SCSC, SSSF, SFSF, and SCSF plates. The integrated equations of motion in terms of the stress resultant are derived based on the first order shear deformation theory.

In this paper the elastic-plastic impact on relatively thick rectangular plate having two opposite edges simply supported and subjected to in-plane loads has been studied. The plate is rested on the Pasternak elastic foundation and the other two edges of the plate can be combinations of classical boundary conditions such as free, simply supported and clamped boundary conditions. In order to reduce the number of the independent parameters involving in the impact process and reduction of computation time, equations of motion are presented in the dimensionless form [23]. The Reissner-Mindlin plate theory which considers the first-order shear deformation and rotary inertia effects is used to derive the dimensionless equations of motion. The exact closed form solutions of mode shape functions which are presented in [22] are used to study the behavior of the plate subjected to impulsive load. To solve the force time history resulting from the elastic-plastic impact, the time increment method is used.

2 Governing equations of moderately thick plate

Consider a flat, isotropic, moderately thick rectangular plate of length a, width b, uniform thickness h, modulus of Elasticity E_p, Poisson's ratio υ_p, and density ρ, oriented so that its undeformed middle surface contains the x_1 and x_2-axis of a Cartesian coordinate system (x_1, x_2, x_3), subjected to uniformly biaxial in-plane loads as illustrated in Fig. 1. Two edges of the plate parallel to the x_2-axis are assumed to be simply supported while the other two can be combination of free, simply supported, or clamped boundary conditions as shown in Fig. 2.
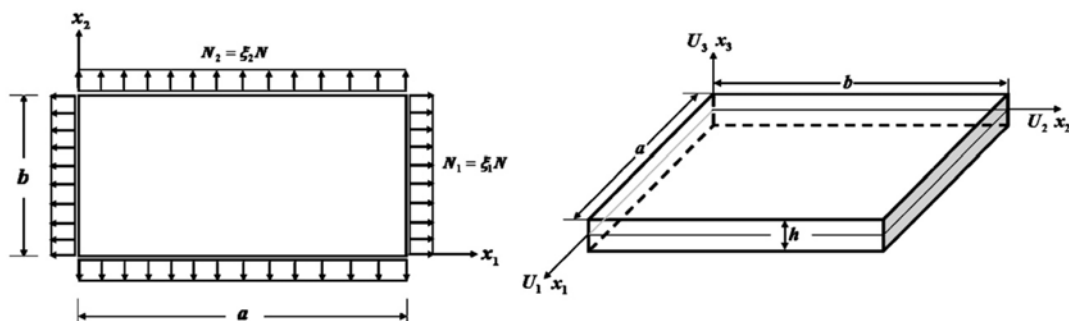

Figure 1 Moderately thick rectangular plate under biaxial in-plane loads and co-ordinate convention
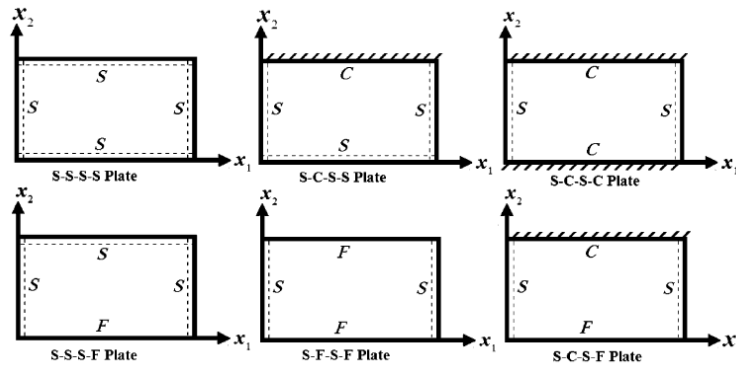
Figure 2 Boundary conditions

The governing differential equations of motion based on the Mindlin first order shear deformation theory as given in [22] are

$$M_{11,1} + M_{12,2} - Q_1 = -(1/12)\rho h^3 \ddot{\psi}_1 \tag{1-a}$$

$$M_{12,1} + M_{22,2} - Q_2 = -(1/12)\rho h^3 \ddot{\psi}_2 \tag{1-b}$$

$$Q_{1,1} + Q_{2,2} + p = \rho h \ddot{\psi}_3 \tag{1-c}$$

where ψ_1, ψ_2 are the rotations of the transverse normal about x_2 and x_1-axis, respectively and ψ_3 is the transverse displacement. Also, M_{11} and M_{22} are the bending moments, M_{12} is the twisting moment, Q_1 and Q_2 are the transverse shear forces, all per unit length which may be written as

$$M_{11} = -D\left(\psi_{1,1} + \upsilon_p\psi_{2,2}\right) \tag{2-a}$$

$$M_{22} = -D\left(\psi_{2,2} + \upsilon_p\psi_{1,1}\right) \tag{2-b}$$

$$M_{12} = -\frac{D}{2}\left(1-\upsilon_p\right)\left(\psi_{1,2} + \psi_{2,1}\right) \tag{2-c}$$

$$Q_1 = -\kappa^2 Gh\left(\psi_1 + \psi_{3,1}\right) \tag{2-d}$$

$$Q_2 = -\kappa^2 Gh\left(\psi_2 + \psi_{3,2}\right) \tag{2-e}$$

where $D = (E_p h^3)/[12(1-\upsilon_p^2)]$ is the flexural rigidity, $G = E_p/[2(1+\upsilon_p)]$ is the shear rigidity, and κ^2 is the shear correction factor to account for the fact that the transverse shear strains are not fully independent of the thickness coordinate. Substituting Eqs. $(2-a)$ to $(2-e)$ into Eqs. $(1-a)$ to $(1-c)$ gives

$$D\left[\upsilon_1(\psi_{1,11} + \psi_{1,22}) + \upsilon_2(\psi_{1,11} + \psi_{2,12})\right] - \kappa^2 Gh(\psi_1 - \psi_{3,1}) = (1/12)\rho h^3 \ddot{\psi}_1 \tag{3-a}$$

$$D\left[\upsilon_1(\psi_{2,11} + \psi_{2,22}) + \upsilon_2(\psi_{1,12} + \psi_{2,22})\right] - \kappa^2 Gh(\psi_2 - \psi_{3,2}) = (1/12)\rho h^3 \ddot{\psi}_2 \tag{3-b}$$

$$\kappa^2 Gh\left[\psi_{3,11} + \psi_{3,22} - \psi_{1,1} - \psi_{2,2}\right] + K_2\left[\psi_{3,11} + \psi_{3,22}\right] + p - K_1\psi_3 + N_1\psi_{3,11} + N_2\psi_{3,22}$$
$$= \rho h \ddot{\psi}_3 \tag{3-c}$$

where υ_1, υ_2 are defined as

$$\upsilon_1 = \left(1 - \upsilon_p\right)/2, \upsilon_2 = \left(1 + \upsilon_p\right)/2 \tag{4}$$

In order to investigate the effect of impact parameters on plate it is more appropriate to express the governing equations of motion in dimensionless form. In other words the number of independent parameters can be reduced by combining them in non-dimensional groups which in turn minimize the time of computations required. Further, it would help in generalizing and correlating experimental results through the use of minimum amount of data and model test [23]. Thus for generality and convenience, the coordinates are normalized with respect to the plate planar dimensions and the following non-dimensional terms are introduced

$$X_1 = x_1/a, \quad X_2 = x_2/b, \quad \bar{\psi}_1 = a\,\psi_1/\alpha_{max}, \quad \bar{\psi}_2 = a\,\psi_2/\alpha_{max}, \quad \bar{\psi}_3 = \psi_3/\alpha_{max},$$
$$\delta = h/a, \quad \eta = a/b, \quad \beta = \omega/\varphi, \quad \tau = \varphi\, t \tag{5}$$

$$\tilde{N}_1 = \frac{N_1}{a^2\rho h \varphi^2}, \quad \tilde{N}_2 = \frac{N_2}{a^2\rho h \varphi^2}, \quad \tilde{K}_1 = \frac{K_1}{\rho h \varphi^2}, \quad \tilde{K}_2 = \frac{K_2}{a^2\rho h \varphi^2} \tag{6}$$

where β is the frequency parameter, α_{max} is the maximum elastic indention and φ is the normalized time parameter. Introducing the dimensionless parameters given by Eqs. (5) and (6), in Eqs. $(3-a)$ to $(3-b)$ and assuming the free harmonic motion as :

$$\bar{\psi}_1(X_1, X_2, \tau) = \tilde{\psi}_1(X_1, X_2)\ e^{i\beta\tau} \tag{7-a}$$

$$\bar{\psi}_1(X_1, X_2, \tau) = \tilde{\psi}_1(X_1, X_2)\ e^{i\beta\tau} \tag{7-b}$$

$$\bar{\psi}_1(X_1, X_2, \tau) = \tilde{\psi}_1(X_1, X_2)\ e^{i\beta\tau} \tag{7-c}$$

The dimensionless equation of motion for the free vibration of the plate under absence of the load may be expressed as

$$\lambda \left[\ \tilde{\psi}_{1,11} + \eta^2\tilde{\psi}_{1,22} + (\upsilon_2/\upsilon_1)\ \left(\tilde{\psi}_{1,11} + \eta\tilde{\psi}_{2,12}\right)\ \right] - (12\kappa^2\lambda/\delta^2)\ \left(\tilde{\psi}_1 - \tilde{\psi}_{3,1}\right) = -\beta^2\tilde{\psi}_1 \tag{8-a}$$

$$\lambda \left[\ \tilde{\psi}_{2,11} + \eta^2\tilde{\psi}_{2,22} + (\upsilon_2/\upsilon_1)\ \eta\ \left(\tilde{\psi}_{1,12} + \eta\tilde{\psi}_{2,22}\right)\ \right] - (12\kappa^2\lambda/\delta^2)\ \left(\tilde{\psi}_2 - \eta\tilde{\psi}_{3,2}\right)$$
$$= -\beta^2\tilde{\psi}_2 \tag{8-b}$$

$$\left(\kappa^2\lambda + \tilde{K}_2 + \tilde{N}_1\right)\ \tilde{\psi}_{3,11} + \left(\kappa^2\lambda + \tilde{K}_2 + \tilde{N}_2\right)\ \eta^2\tilde{\psi}_{3,22} - \kappa^2\lambda\ \left(\tilde{\psi}_{1,1} + \eta\tilde{\psi}_{2,2}\right) - \tilde{K}_1\ \tilde{\psi}_3$$
$$= -\beta^2\tilde{\psi}_3 \tag{8-c}$$

where $\lambda = (12D\upsilon_1)/(\rho h^3 a^2 \varphi^2)$ is the impact parameter. For the sake of definiteness the dimensionless boundary conditions will be given below for an edge parallel to the X_2-normalized axis. For a simply supported edge

$$\tilde{\psi}_2 = 0, \quad \tilde{\psi}_3 = 0, \quad \tilde{M}_{11} = 0 \tag{9}$$

for a free edge

$$\tilde{M}_{11} = 0, \quad \tilde{M}_{12} = 0, \quad \tilde{Q}_1 = 0 \tag{10}$$

and for a clamped edge

$$\tilde{\psi}_1 = 0, \quad \tilde{\psi}_2 = 0, \quad \tilde{\psi}_3 = 0 \tag{11}$$

Upon making use of the non-dimensional terms the dimensionless equations of moments and transverse shear forces per unit length may be written as :

$$\tilde{M}_{11} = -\left(\tilde{\psi}_{1,1} + \upsilon_p \eta \tilde{\psi}_{2,2}\right) e^{i\beta\tau} \tag{12-a}$$

$$\tilde{M}_{22} = -\left(\eta \tilde{\psi}_{2,2} + \upsilon_p \tilde{\psi}_{1,1}\right) e^{i\beta\tau} \tag{12-b}$$

$$\tilde{M}_{12} = -\upsilon_1 \left(\tilde{\psi}_{1,2} + \tilde{\psi}_{2,1}\right) e^{i\beta\tau} \tag{12-c}$$

$$\tilde{Q}_1 = -\left(\tilde{\psi}_1 + \tilde{\psi}_{3,1}\right) e^{i\beta\tau} \tag{12-d}$$

$$\tilde{Q}_2 = -\left(\tilde{\psi}_2 + \tilde{\psi}_{3,2}\right) e^{i\beta\tau} \tag{12-e}$$

The three dimensionless governing Eqs. (8-a)-(8-c) may be solved by representing the three dimensionless functions $\tilde{\psi}_1$, $\tilde{\psi}_2$ and $\tilde{\psi}_3$ in terms of the three dimensionless potentials W_1, W_2 and W_3 as follow [22]:

$$\tilde{\psi}_1 = C_1 W_{1,1} + C_2 W_{2,1} - \eta W_{3,2} \tag{13-a}$$

$$\tilde{\psi}_2 = C_1 \eta W_{1,2} + C_2 \eta W_{2,2} - W_{1,2} \tag{13-b}$$

$$\tilde{\psi}_3 = W_1 + W_2 \tag{13-c}$$

where

$$C_1 = \frac{12\kappa^2 \upsilon_1 / \delta^2}{\left(\tilde{\alpha}_1^2 - \upsilon_1 \tilde{\alpha}_3^2\right)} = \frac{a_1 \mu^2 + a_2 \eta^2 \theta_1^2 - a_3}{\tilde{\alpha}_1^2}$$

$$C_2 = \frac{12\kappa^2 \upsilon_1 / \delta^2}{\left(\tilde{\alpha}_2^2 - \upsilon_1 \tilde{\alpha}_3^2\right)} = \frac{a_1 \mu^2 + a_2 \eta^2 \theta_2^2 - a_3}{\tilde{\alpha}_2^2} \tag{14}$$

$$\theta_1^2 = \frac{-\theta + \sqrt{\theta^2 - 4\tilde{\alpha}}}{2}, \quad \theta_2^2 = \frac{-\theta + \sqrt{\theta^2 - 4\tilde{\alpha}}}{2},$$

$$\tilde{\alpha}_3^2 = \frac{\kappa^2 \lambda}{\beta^2 \upsilon_1} \quad \tilde{\alpha}_1^2 \tilde{\alpha}_2^2 = \frac{\beta^2}{\lambda} - \frac{12\kappa^2}{\delta^2}, \quad \theta_3^2 = \frac{1}{\eta^2}\left(m^2\pi^2 - \frac{\beta^2}{\lambda} + \frac{12\kappa^2}{\delta^2}\right) \tag{15}$$

$$\theta = \frac{a_1 \mu^2 + a_2 \mu^2 - a_3 - a_5}{a_2 \eta^2}, \quad \tilde{\alpha} = \frac{a_1 \mu^4 - \left(a_3 + a_4\right)\mu^2 + a_6}{a_2 \eta^4}, \tag{16}$$

and $a_i (i = 1, 2, \cdots, 6)$ are constant coefficients as

$$a_1 = 1 + \frac{\tilde{N}_1}{\kappa^2 \lambda} + \frac{\tilde{K}_2}{\kappa^2 \lambda} \tag{17-a}$$

$$a_2 = 1 + \frac{\tilde{N}_2}{\kappa^2 \lambda} + \frac{\tilde{K}_2}{\kappa^2 \lambda} \tag{17-b}$$

$$a_3 = \frac{1}{\kappa^2 \lambda}\left(\beta^2 - \tilde{K}_1\right) \tag{17-c}$$

$$a_4 = \frac{\beta^2 \upsilon_1}{\lambda} + \left(\frac{\beta^2 \upsilon_1}{\kappa^2 \lambda^2} - \frac{12\upsilon_1}{\delta^2 \lambda}\right)\left(\tilde{N}_1 + \tilde{K}_2\right) \tag{17-d}$$

$$a_5 = \frac{\beta^2 \upsilon_1}{\lambda} + \left(\frac{\beta^2 \upsilon_1}{\kappa^2 \lambda^2} - \frac{12\upsilon_1}{\delta^2 \lambda}\right)\left(\tilde{N}_2 + \tilde{K}_2\right) \tag{17-e}$$

$$a_6 = \left(\frac{\beta^2 \upsilon_1}{\kappa^2 \lambda^2} - \frac{12\upsilon_1}{\delta^2 \lambda}\right)\left(\beta^2 - \tilde{K}_1\right) \tag{17-f}$$

The general solution of differential Eqs. $(8-a)$ to $(8-c)$ in terms of W_1, W_2 and W_3 can be expressed as

$$W_{1,11} + \eta^2 W_{1,22} = \tilde{\alpha}_1^2 W_1 \tag{18-a}$$

$$W_{2,11} + \eta^2 W_{2,22} = \tilde{\alpha}_2^2 W_2 \tag{18-b}$$

$$W_{3,11} + \eta^2 W_{3,22} = \tilde{\alpha}_3^2 W_3 \tag{18-c}$$

Solutions of the above equations based on [22] are taken as :

$$W_1 = \left[A_1 \sin\left(\theta_1 X_2\right) + A_2 \cos\left(\theta_1 X_2\right)\right]\sin\left(\mu X_1\right) \tag{19-a}$$

$$W_2 = \left[A_3 \sin\left(\theta_2 X_2\right) + A_4 \cos\left(\theta_2 X_2\right)\right]\sin\left(\mu X_1\right) \tag{19-b}$$

$$W_3 = \left[A_5 \sin\left(\theta_3 X_2\right) + A_6 \cos\left(\theta_3 X_2\right)\right]\cos\left(\mu X_1\right) \tag{19-c}$$

In which arbitrary constants $A_i(i=1,2,\ldots 6)$, $\theta_j(j=1,2,3)$, and $\mu = m\,\pi\,(m=1,2,3)$ are related to $\tilde{\alpha}_i$ by

$$\tilde{\alpha}_1^2 = \mu_1^2 + \eta^2 \theta_1^2, \quad \tilde{\alpha}_2^2 = \mu_2^2 - \eta^2 \theta_2^2, \quad \tilde{\alpha}_3^2 = \mu_3^2 - \eta^2 \theta_3^2 \tag{20}$$

Introducing Eqs. (19) in Eqs. (13) together with utilizing Eqs. (14-16), and substituting the results into the three appropriate boundary conditions along the edges $X_2 = 0$ and $X_2 = 1$ lead to a characteristic determinant of the six order for each m. Expanding determinant and collecting terms yields a characteristic equation for any appropriate boundary conditions that illustrated in Fig. 2.

3 Forced vibration solution

The eigenvalue expansion method may now be used to obtain the response of the plate subjected to impulsive load. For this purpose Eqs. (3-a) to (3-c) may be written in dimensionless form as :

$$\bar{\psi}_{1,11} + \eta^2 \bar{\psi}_{1,22} + (\nu_2/\nu_1)\left(\bar{\psi}_{1,11} + \eta\bar{\psi}_{2,12}\right) - (12\kappa^2/\delta^2)\left(\bar{\psi}_1 - \bar{\psi}_{3,1}\right) = \frac{1}{\lambda}\ddot{\bar{\psi}}_1 \tag{21-a}$$

$$\bar{\psi}_{2,11} + \eta^2 \bar{\psi}_{2,22} + (\upsilon_2 / \upsilon_1)\eta\left(\bar{\psi}_{1,12} + \eta\bar{\psi}_{2,22}\right) - (12\kappa^2 / \delta^2)\left(\bar{\psi}_2 - \eta\bar{\psi}_{3,2}\right) = \frac{1}{\lambda}\ddot{\bar{\psi}}_2 \qquad (21\text{-}b)$$

$$\left(\kappa^2\lambda + \tilde{K}_2 + \tilde{N}_1\right)\bar{\psi}_{3,11} + \left(\kappa^2\lambda + \tilde{K}_2 + \tilde{N}_2\right)\eta^2\bar{\psi}_{3,22} - \kappa^2\lambda\left(\bar{\psi}_{1,1} + \eta\bar{\psi}_{2,2}\right) - \tilde{K}_1\bar{\psi}_3 + \bar{p} = \ddot{\bar{\psi}}_3 \qquad (21\text{-}c)$$

where $\bar{p}\left(X_1, X_2, \tau\right) = \dfrac{p\left(x_1, x_2, t\right)}{\rho h \varphi^2 \alpha_{\max}}$ is the non-dimensional impact force. Thus the response of

the plate to the $\bar{p}\left(X_1, X_2, \tau\right)$ according to the eigenvalue expansion method may be assumed

to be

$$\bar{\psi}_1(X_1, X_2, \tau) = \sum_{m=1}^{\infty}\sum_{n=1}^{\infty} \bar{\bar{\psi}}_1^{mn}(X_1, X_2)T^{mn}(\tau) \qquad (22\text{-}a)$$

$$\bar{\psi}_2(X_1, X_2, \tau) = \sum_{m=1}^{\infty}\sum_{n=1}^{\infty} \bar{\bar{\psi}}_2^{mn}(X_1, X_2)T^{mn}(\tau) \qquad (22\text{-}b)$$

$$\bar{\psi}_3(X_1, X_2, \tau) = \sum_{m=1}^{\infty}\sum_{n=1}^{\infty} \bar{\bar{\psi}}_3^{mn}(X_1, X_2)T^{mn}(\tau) \qquad (22\text{-}c)$$

where $\bar{\bar{\psi}}_1^{mn}(X_1, X_2), \bar{\bar{\psi}}_2^{mn}(X_1, X_2)$, and $\bar{\bar{\psi}}_3^{mn}(X_1, X_2)$, are the vibrational mode-shape functions. Also n, m are numbers of semi-waves in directions of X_1, X_2 axis and $T^{mn}(\tau)$ are the corresponding time functions associated with the mode-shape functions. Substituting Eqs. (22-a) to (22-c) into Eqs. (21-a) to (21-c) gives

$$\sum_{m=1}^{\infty}\sum_{n=1}^{\infty}\left[\bar{\bar{\psi}}_{1,11}^{mn} + \eta^2\bar{\bar{\psi}}_{1,22}^{mn} + \frac{\upsilon_2}{\upsilon_1}\left(\bar{\bar{\psi}}_{1,22}^{mn} + \eta\bar{\bar{\psi}}_{2,12}^{mn}\right) - \frac{12\kappa^2}{\delta^2}\left(\bar{\bar{\psi}}_1^{mn} - \bar{\bar{\psi}}_{3,1}^{mn}\right)\right] T^{mn}(\tau)$$
$$= \frac{1}{\lambda}\sum_{m=1}^{\infty}\sum_{n=1}^{\infty} \bar{\bar{\psi}}_1^{mn}(X_1, X_2)\ddot{T}^{mn}(\tau) \qquad (23\text{-}a)$$

$$\sum_{m=1}^{\infty}\sum_{n=1}^{\infty}\left[\bar{\bar{\psi}}_{2,11}^{mn} + \eta^2\bar{\bar{\psi}}_{2,22}^{mn} + \frac{\upsilon_2}{\upsilon_1}\eta\left(\bar{\bar{\psi}}_{1,12}^{mn} + \eta\bar{\bar{\psi}}_{2,22}^{mn}\right) - \frac{12\kappa^2}{\delta^2}\left(\bar{\bar{\psi}}_2^{mn} - \eta\bar{\bar{\psi}}_{3,2}^{mn}\right)\right] T^{mn}(\tau)$$
$$= \frac{1}{\lambda}\sum_{m=1}^{\infty}\sum_{n=1}^{\infty} \bar{\bar{\psi}}_2^{mn}(X_1, X_2)\ddot{T}^{mn}(\tau) \qquad (23\text{-}b)$$

$$\sum_{m=1}^{\infty}\sum_{n=1}^{\infty}\left[\left(\kappa^2\lambda + \tilde{K}_2 + \tilde{N}_1\right)\bar{\bar{\psi}}_{3,11}^{mn} + \left(\kappa^2\lambda + \tilde{K}_2 + \tilde{N}_2\right)\eta^2\bar{\bar{\psi}}_{3,22}^{mn} - \kappa^2\lambda\left(\bar{\bar{\psi}}_{1,1}^{mn} + \eta\bar{\bar{\psi}}_{2,2}^{mn}\right)\right.$$
$$\left. - \tilde{K}_1\bar{\bar{\psi}}_3^{mn}\right] T^{mn}(\tau) + \bar{p} = \sum_{m=1}^{\infty}\sum_{n=1}^{\infty} \bar{\bar{\psi}}_3^{mn}(X_1, X_2)\ddot{T}^{mn}(\tau) \qquad (23\text{-}c)$$

The vibrational mode shape functions also satisfy the free vibration Eqs. (8-a)-(8-c). Hence

$$\bar{\bar{\psi}}_{1,11}^{mn} + \eta^2\bar{\bar{\psi}}_{1,22}^{mn} + \frac{\upsilon_2}{\upsilon_1}\left(\bar{\bar{\psi}}_{1,22}^{mn} + \eta\bar{\bar{\psi}}_{2,12}^{mn}\right) - \frac{12\kappa^2}{\delta^2}\left(\bar{\bar{\psi}}_1^{mn} - \bar{\bar{\psi}}_{3,1}^{mn}\right) = -\frac{\left(\beta^{mn}\right)^2}{\lambda}\bar{\bar{\psi}}_1^{mn} \qquad (24\text{-}a)$$

$$\bar{\bar{\psi}}_{2,11}^{mn} + \eta^2\bar{\bar{\psi}}_{2,22}^{mn} + \frac{\upsilon_2}{\upsilon_1}\eta\left(\bar{\bar{\psi}}_{1,12}^{mn} + \eta\bar{\bar{\psi}}_{2,22}^{mn}\right) - \frac{12\kappa^2}{\delta^2}\left(\bar{\bar{\psi}}_2^{mn} - \eta\bar{\bar{\psi}}_{3,2}^{mn}\right) = -\frac{\left(\beta^{mn}\right)^2}{\lambda}\bar{\bar{\psi}}_2^{mn} \qquad (24\text{-}b)$$

$$\left(\kappa^2\lambda + \tilde{K}_2 + \tilde{N}_1\right)\,\overline{\overline{\psi}}_{3,11}^{mn} + \left(\kappa^2\lambda + \tilde{K}_2 + \tilde{N}_2\right)\,\eta^2\overline{\overline{\psi}}_{3,22}^{mn} - \kappa^2\lambda\left(\overline{\overline{\psi}}_{1,1}^{mn} + \eta\overline{\overline{\psi}}_{2,2}^{mn}\right) - \tilde{K}_1\overline{\overline{\psi}}_3^{mn}$$
$$= -\left(\beta^{mn}\right)^2\overline{\overline{\psi}}_3^{mn} \tag{24-c}$$

Substituting from Eqs. (24-a) to (24-c) into Eqs. (23-a)-(23-c) gives

$$-\sum_{m=1}^{\infty}\sum_{n=1}^{\infty}\left[\left(\beta^{mn}\right)^2\overline{\overline{\psi}}_1^{mn}\right]T^{mn}(\tau) = \sum_{m=1}^{\infty}\sum_{n=1}^{\infty}\overline{\overline{\psi}}_1^{mn}(X_1,X_2)\ddot{T}^{mn}(\tau) \tag{25-a}$$

$$-\sum_{m=1}^{\infty}\sum_{n=1}^{\infty}\left[\left(\beta^{mn}\right)^2\overline{\overline{\psi}}_2^{mn}\right]T^{mn}(\tau) = \sum_{m=1}^{\infty}\sum_{n=1}^{\infty}\overline{\overline{\psi}}_2^{mn}(X_1,X_2)\ddot{T}^{mn}(\tau) \tag{25-b}$$

$$-\sum_{m=1}^{\infty}\sum_{n=1}^{\infty}\left[\left(\beta^{mn}\right)^2\overline{\overline{\psi}}_3^{mn}\right]T^{mn}(\tau) + \overline{p} = \sum_{m=1}^{\infty}\sum_{n=1}^{\infty}\overline{\overline{\psi}}_3^{mn}(X_1,X_2)\ddot{T}^{mn}(\tau) \tag{25-c}$$

Upon making use of the orthogonality of the mode-shape functions and some aljebric manipulations, Eqs. (25-a)-(25-c) may be combined to give a single equation as :

$$\ddot{T}^{mn}(\tau)\int_0^1\int_0^1\left[\frac{\delta^2}{12}\left(\left(\overline{\overline{\psi}}_1^{mn}\right)^2+\left(\overline{\overline{\psi}}_2^{mn}\right)^2\right)+\left(\overline{\overline{\psi}}_3^{mn}\right)^2\right]dX_1dX_2 + \left(\beta^{mn}\right)^2 T^{mn}(\tau)\times$$
$$\int_0^1\int_0^1\left[\frac{\delta^2}{12}\left(\left(\overline{\overline{\psi}}_1^{mn}\right)^2+\left(\overline{\overline{\psi}}_2^{mn}\right)^2\right)+\left(\overline{\overline{\psi}}_3^{mn}\right)^2\right]dX_1dX_2 = \int_0^1\int_0^1 \overline{p}\,\overline{\overline{\psi}}_3^{mn}dX_1dX_2 \tag{26}$$

By introducing

$$K^{mn} = \int_0^1\int_0^1\left[\left(\delta^2/12\right)\left(\left(\overline{\overline{\psi}}_1^{mn}\right)^2+\left(\overline{\overline{\psi}}_2^{mn}\right)^2\right)+\left(\overline{\overline{\psi}}_3^{mn}\right)^2\right]dX_1dX_2, \tag{27}$$

$$Q^{mn}(\tau) = \int_0^1\int_0^1 \overline{p}\,\overline{\overline{\psi}}_3\,dX_1dX_2, \tag{28}$$

Eq. (26) may now be written as

$$\ddot{T}^{mn}(\tau) + \left(\beta^{mn}\right)^2 T^{mn}(\tau) = Q^{mn}(\tau)/K^{mn} \tag{29}$$

Solving Eq. (29) by using the Laplace transform method yields

$$T^{mn}(\tau) = \frac{1}{K^{mn}\beta^{mn}}\int_0^\tau Q^{mn}(\Gamma)\sin\left[\beta^{mn}(t-\Gamma)\right]d\Gamma + T^{mn}(0)\cos\left(\beta^{mn}\tau\right)$$
$$+ \frac{\sin\left(\beta^{mn}\tau\right)}{\beta^{mn}}\dot{T}^{mn} \tag{30}$$

By assuming the initial conditions as

$$\left.\left(\overline{\psi}_1,\overline{\psi}_2,\overline{\psi}_3\right)\right|_{\tau=0}=0, \quad \left.\left(\partial\psi_1/\partial\tau,\partial\psi_2/\partial\tau,\partial\psi_3/\partial\tau\right)\right|_{\tau=0}=0 \Rightarrow \begin{cases} T^{mn}(0)=0 \\ \dot{T}^{mn}(0)=0 \end{cases} \tag{31}$$

we obtain

$$T^{mn}(\tau) = \frac{1}{K^{mn}\beta^{mn}} \int_0^\tau Q^{mn}(\Gamma) \sin\left[\beta^{mn}(t-\tau)\right] d\Gamma \tag{32}$$

Thus the response of the plate subjected to the impact load in transverse direction may be obtained by substituting Eq. (32) into Eq. (22-c).

$$\bar{\psi}_3(X_1, X_2, \tau) = \sum_{m=1}^\infty \sum_{n=1}^\infty \frac{\bar{\bar{\psi}}_3^{mn}(X_1, X_2)}{K^{mn}\beta^{mn}} \int_0^\tau Q^{mn}(\Gamma) \sin\left[\beta^{mn}(t-\tau)\right] d\Gamma \tag{33}$$

4 Normalization of impact equations

In the impact problems where the contact duration is long in comparison with the wave period, the static contact laws such as one given in Eq. (34) can be used for problems involving moderate impact velocities [24]. According to the Hertz theory of contact the relationship between the force and indentation in contact of two elastic bodies may be given by

$$F = k_2 \alpha^{(3/2)} \quad 0 \le \alpha \le \alpha_{max} \tag{34}$$

where

$$k_2 = (4/3)\sqrt{R_i}E^*, \quad 1/E^* = \left(1 - \upsilon_i^2\right)/E_i + \left(1 - \upsilon_p^2\right)/E_p, \tag{35}$$

and υ_i, E_i are Poisson ratio and Young modulus of impactor respectively. Consider now collision of a spherical object having initial velocity V_0 with a plate initially at rest as shown in Fig. 3.
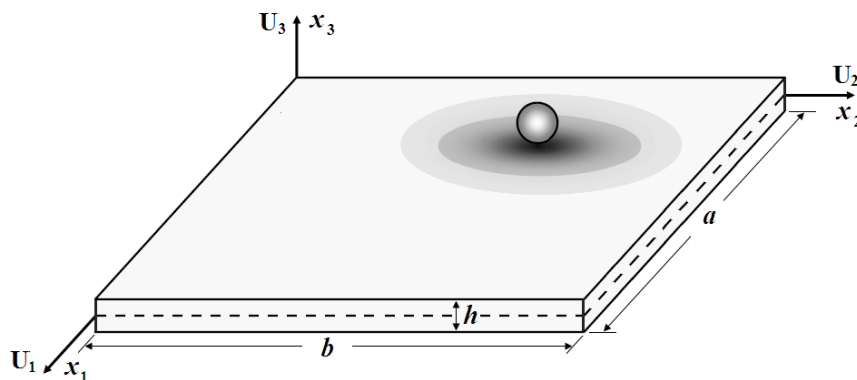

Figure 3 Impact of an object on plate

Knowing that the maximum indentation can occur when the relative velocity $\dot{\alpha}$ is zero and using $\ddot{\alpha}d\alpha = \dot{\alpha}d\dot{\alpha}$, the maximum indentation can be represented as :

$$\alpha_{max} = \left(\frac{5m_i}{4k_2}V_0^2\right)^{2/5} \tag{36}$$

That is the precise upper limit of the indentation for the low velocity impact [28]. The displacement of the impactor may also be given in dimensionless form as

$$\bar{\psi}_i = \psi_i / \alpha_{max} \tag{37}$$

where $\bar{\psi}_i$ is the dimensionless displacement of the impactor. Using Newton's 2nd law together with the dimensionless time $\tau = \varphi\, t$, it is not difficult to show that

$$\ddot{\bar{\psi}}_i = -F(t) / (m_i \alpha_{max} \varphi^2) = -\bar{F}(\tau) \tag{38}$$

Introducing $\bar{\alpha} = \alpha / \alpha_{max}$ and using equation (34) gives

$$\bar{F}(\tau) = k_2 \alpha^{(3/2)} / (m_i \alpha_{max} \varphi^2) = k_2 \sqrt{\alpha_{max}}\, \bar{\alpha}^{(3/2)} / (m_i \varphi^2) \tag{39}$$

The non-dimensional impact force given by Eq. (38) may be normalized by introducing

$$\varphi^2 = k_2 \sqrt{\alpha_{max}} / m_i \tag{40}$$

Thus the dimensionless form of force-indentation relationship for elastic collisions may be given by

$$\bar{F}(\tau) = (\bar{\alpha})^{(3/2)} \quad 0 \leq \bar{\alpha} \leq 1 \tag{41}$$

4-1 Elastic-plastic contact law

If the stress resulting from the impact of the object on the plate is more than the Yield strength of the plate, the Hertz impact theory can no longer be used to predict result. This is because of generation of the permanent indentation which is on contrast with the elastic assumption. Based on the elastic-plastic contact law [24], the contact interval is viewed as consisting of three periods:

1- An initial elastic compression according to the Hertz law of contact. Thus in this stage equation $F = k_2 \alpha^{(3/2)}$ may be used until a given critical stress q_0 is first attained.

2- The indentation that is started from the end of the first stage and during which a plastic zone enclosed by an elastic ring moves outward from the center of the area of contact under constant stress q_0.

3- A restitution initiated when the relative velocity of two objects is zero and involving restoration of the accumulated elastic strain energy.

During the first stage we may write

$$F = k_2 \alpha^{(3/2)} \quad 0 \leq \alpha \leq \alpha_1, \quad \alpha_1 = \frac{\pi^2 R_i q_0^2}{4\left(E^*\right)^2} \tag{42}$$

where α_1 and R_i are the indentation at the end of first stage and radius of impactor respectively. The dimensionless impact force can also be given by

$$\bar{F}(\tau) = (\bar{\alpha})^{(3/2)} \quad 0 \leq \bar{\alpha} \leq \bar{\alpha}_1 \tag{43}$$

where $\bar{\alpha} = \alpha_1 / \alpha_{max}$. The non-dimensional form of force during the second and third stages as shown in [23] are

$$\overline{F}(\tau) = (3\overline{\alpha} - 1)/2 \qquad 1 \le \overline{\alpha} \le \overline{\alpha}_2 \tag{44}$$

$$\overline{F}(\tau) = \frac{3}{2}\left[(\overline{\alpha}_2 - 1)\sqrt{\overline{\alpha} - \overline{\alpha}_2 + 1} + \frac{2}{3}\sqrt[3]{(\overline{\alpha} - \overline{\alpha}_2 + 1)^2}\right] \tag{45}$$

Having the response of the plate to a typical force $\overline{p}(X_1, X_2, \tau)$ as given by Eq. (33), the transverse response of the plate to the impact load applied at position $X_1 = \overline{X}_1$ and $X_1 = \overline{X}_2$

$$\overline{p}(\overline{X}_2, \overline{X}_2, \tau) = \overline{m}\,\overline{F}(\tau)\,\delta(X_1 - \overline{X}_1)\,\delta(X_2 - \overline{X}_2), \quad \overline{m} = m_i/m_p \tag{46}$$

may be written as :

$$\overline{\psi}_3(X_1, X_2, \tau) = \sum_{m=1}^{\infty}\sum_{n=1}^{\infty}\frac{\overline{m}\,\overline{\overline{\psi}}_3^{mn}(X_1, X_2)}{K^{mn}\beta^{mn}}\int_0^{\tau}\overline{F}(\tau)\sin\left[\beta^{mn}(\tau - \Gamma)\right]d\Gamma$$
$$\times\int_0^1\int_0^1\delta(X_1 - \overline{X}_1)\,\delta(X_2 - \overline{X}_2)\,\overline{\overline{\psi}}_3^{mn}(X_1, X_2)dX_1dX_2 \tag{47}$$

where the Dirac delta functions, $\delta(X_1 - \overline{X}_1)$ and $\delta(X_2 - \overline{X}_2)$ presenting the position of the applied load on the plate. The integral involving Dirac delta functions on the right-hand side of Eq. (47) may be simplified as

$$\int_0^1\int_0^1\delta(X_1 - \overline{X}_1)\delta(X_2 - \overline{X}_2)\,\overline{\overline{\psi}}_3^{mn}(X_1, X_2)dX_1dX_2 = \overline{\overline{\psi}}_3^{mn}(\overline{X}_1, \overline{X}_2) \tag{48}$$

Hence, the transverse response of the plate to the impulsive load acting at $X_1 = \overline{X}_1, X_2 = \overline{X}_2$ can be written as :

$$\overline{\psi}_3(X_1, X_2, \tau) = \sum_{m=1}^{\infty}\sum_{n=1}^{\infty}\frac{\overline{m}\,\overline{\overline{\psi}}_3^{mn}(X_1, X_2)\,\overline{\overline{\psi}}_3^{mn}(\overline{X}_1, \overline{X}_2)}{K^{mn}\beta^{mn}}\int_0^{\tau}\overline{F}(\tau)\sin\left[\beta^{mn}(\tau - \Gamma)\right]d\Gamma \tag{49}$$

Also after some simple aljebric manipulation the impact parameter λ appearing first in Eqs. (8-a)-(8-c) can be given by

$$\lambda = \left(\frac{3}{4\pi^{1/5}2^{3/5}5^{1/5}}\right)\left(\frac{E_p}{(1+\upsilon_p)V_0^{2/5}\rho_i^{1/5}}\right)\left(\frac{\overline{m}h}{R_i\eta}\right)\frac{1}{(E^*)^{4/5}} \tag{50}$$

and

$$\lambda = \left(\frac{3}{4\pi(1+\upsilon_p)}\right)\left(\frac{\overline{m}h}{R_i}\right)\frac{1}{\eta}\frac{E_p}{q_0} \tag{51}$$

for the first and second stages of impact process respectively. The initial conditions for the impactor are

$$\overline{\psi}_i(0) = 0, \quad \xi = \frac{d\overline{\psi}_i(t)}{dt}\bigg|_{t=0} = \frac{V_0}{\varphi\,\alpha_{max}} \tag{52}$$

where ξ is the non-dimensional initial velocity. Using the Newton's 2nd law together with the Laplace transformation for the impactor we get

$$\psi_i(\tau) = \xi\tau - \int_0^\tau (\tau - \Gamma) \, \overline{F}(\Gamma) \, d(\Gamma). \tag{53}$$

The non-dimensional indentation at any instance of the contact period may now be given by $\bar{\alpha} = \overline{\psi}_i - \overline{\psi}_3$. Thus

$$\bar{\alpha} = \xi\tau - \sum_{m=1}^{\infty}\sum_{n=1}^{\infty} \overline{m}(\overline{\overline{\psi}}_3(\overline{X}_1, \overline{X}_2))^2 / (K^{mn}\beta^{mn}) \int_0^\tau \overline{F}(\Gamma) \sin\left[\beta^{mn}(\tau - \Gamma)\right] d\Gamma$$
$$- \int_0^\tau \overline{F}(\Gamma)(\tau - \Gamma) d\Gamma. \tag{54}$$

Substituting for $\bar{\alpha}$ from Eqs. (43)-(45) into Eq. (54), the non-dimensional impact force for the three stages of the impact process may be given by

✓ Elastic stage

$$\left(\overline{F}(\tau)\right)^{3/2} = \xi\tau - \sum_{m=1}^{\infty}\sum_{n=1}^{\infty} \overline{m} \, [\overline{\overline{\psi}}_3(\overline{X}_1, \overline{X}_2)]^2 / (K^{mn}\beta^{mn}) \int_0^\tau \overline{F}(\Gamma) \sin\left[\beta^{mn}(\tau - \Gamma)\right] d\Gamma$$
$$- \int_0^\tau \overline{F}(\Gamma)(\tau - \Gamma) d\Gamma \tag{55}$$

✓ Elastic-plastic stage

$$\frac{2\overline{F}(\tau)+1}{3} = \xi\tau - \sum_{m=1}^{\infty}\sum_{n=1}^{\infty} \overline{m} \, [\overline{\overline{\psi}}_3(\overline{X}_1, \overline{X}_2)]^2 / (K^{mn}\beta^{mn}) \int_0^\tau \overline{F}(\Gamma) \sin\left[\beta^{mn}(\tau - \Gamma)\right] d\Gamma$$
$$- \int_0^\tau \overline{F}(\Gamma)(\tau - \Gamma) d\Gamma \tag{56}$$

✓ Elastic unloading phase

$$\bar{\alpha} = \xi\tau - \sum_{m=1}^{\infty}\sum_{n=1}^{\infty} \overline{m} \, [\overline{\overline{\psi}}_3(\overline{X}_1, \overline{X}_2)]^2 / (K^{mn}\beta^{mn}) \int_0^\tau \overline{F}(\Gamma) \sin\left[\beta^{mn}(\tau - \Gamma)\right] d\Gamma$$
$$- \int_0^\tau \overline{F}(\Gamma)(\tau - \Gamma) d\Gamma \tag{57}$$
$$\overline{F}(\tau) = \frac{3}{2}\left[(\bar{\alpha}_2 - 1)\sqrt{\bar{\alpha} - \bar{\alpha}_2 + 1} + \frac{2}{3}\sqrt[3/2]{\bar{\alpha} - \bar{\alpha}_2 + 1}\right]$$

The solution of Eqs. (55)-(57) may be obtained by means of the small increment method where the contact force is regarded as constant during any time increment $\Delta\tau$. The time increment $\Delta\tau$ is conveniently chosen as some small fraction of the fundamental period of vibration of the plate.

5 Convergence study

In order to chose the upper limit of the double summation in Eqs. (55)-(57) the convergency study should be carried out. Reaching to a proper convergency depends on the number of the modes that are used in predicting the structural dynamic response. Also because of using the small increment method, the time increment $\Delta \tau$ could be very important. In this section, we will consider the effect of these two important parameters on the maximum impact force. Using the material properties listed in Table 1 together with the selected time increment $\Delta \tau$ and the number of the modes listed in the second and the third columns of Table 2 predicts the maximum impact force listed in the forth column of Table 2.

Table 1 Assumed Material properties for convergence study

η	δ	υ_p	λ	κ^2	ξ	$\bar{m}$
0.4	0.1	0.3	0.5	0.86667	$2/\sqrt{5}$	0.01

The trend of the calculated impact force shows that a decrease in time increment causes an increase in maximum non-dimensional force. On the contrary an increase in the number of modes causes a decrease in maximum non-dimensional force. Hence based on the result given in Table 2 appropriate convergence can be achieved for $\Delta \tau = 0.005$ and number of modes equals to 1000.

Table 2 Maximum impact force resulted from time increment and number of mode shapes variation

	$\Delta \tau$	*Number of mode shapes*	*Maximum impact force*
Case 1	*0.05*	*100*	*0.884969*
Case 2	*0.05*	*200*	*0.882542*
Case 3	*0.05*	*500*	*0.879779*
Case 4	*0.05*	*1000*	*0.877477*
Case 5	*0.01*	*1000*	*0.894522*
Case 6	*0.005*	*1000*	*0.896666*

It is shown that the percentage of difference for the maximum impact force when the time increment varies from 0.05 to 0.005, is only 2.14% and when the number of modes vary from 100 to 1000, is 0.835% . Note that by reducing the time increment and increasing the number of modes accuracy of the result can be improved, but the calculations time will be increased. In all calculations the time increment and the mode numbers are selected as 0.005 and 3000 respectively.

6 Numerical examples and discussion

In Fig. 4 the force-time history calculated by the present method on a basis of the Hertz law of contact is compared with those given in reference [16] for both the classical and the Mindlin plate theory neglecting the effect of rotary inertia. The plate and impactor properties are taken from [16] and presented in Table 3.

Table 3 The plate and impactor properties

plate	impactor
$E_p = 206.85\,GPa$	$E_i = 206.85\,GPa$
$\upsilon_p = 0.3$	$\upsilon_i = 0.3$
$\rho = 7837\,kg\,/\,m^3$	$\rho_i = 7837\,kg\,/\,m^3$
$a,b : 0.762, 0.0127\,m$	$R_i : 0.0127\,m$

It can be seen that because of the present method take into account the effect of both shear deformation as well as the effect of rotary inertia the maximum impact force diminishes in comparison with the maximum force related to the force-time history given in [16]. Thus neglecting the effect of rotary inertia causes an increase in the maximum force. In Fig. 5, the force-time history calculated by the present method based on the elastic-plastic impact law is compared with the one given in reference [16]. The difference between two curves quite noticeable showing that the theory used in the interpretation of the elastic-plastic contact could play a major rule in reliability of result.

$$F / \left(k_2 h^{3/2} \right)^{1/2}$$

$$t / \left(\rho \, h^{5/2} / k_2 \right)^{1/2}$$
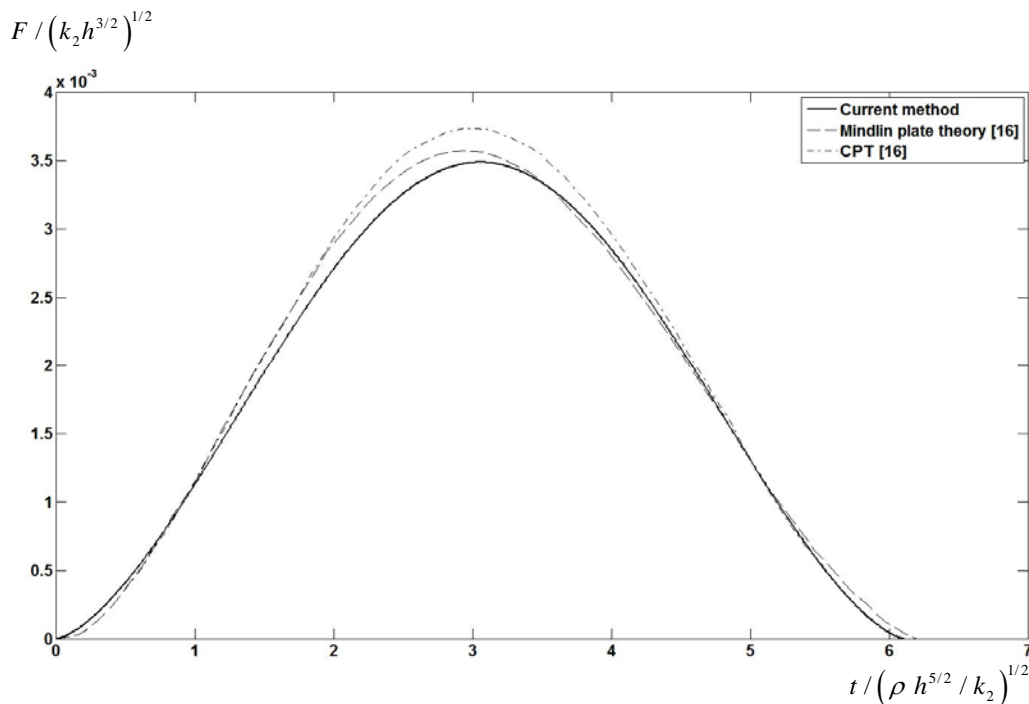
Figure 4 Comparison of result obtained from exact solution of Mindlin theory with result of MPT and CPT given in Ref. [16]
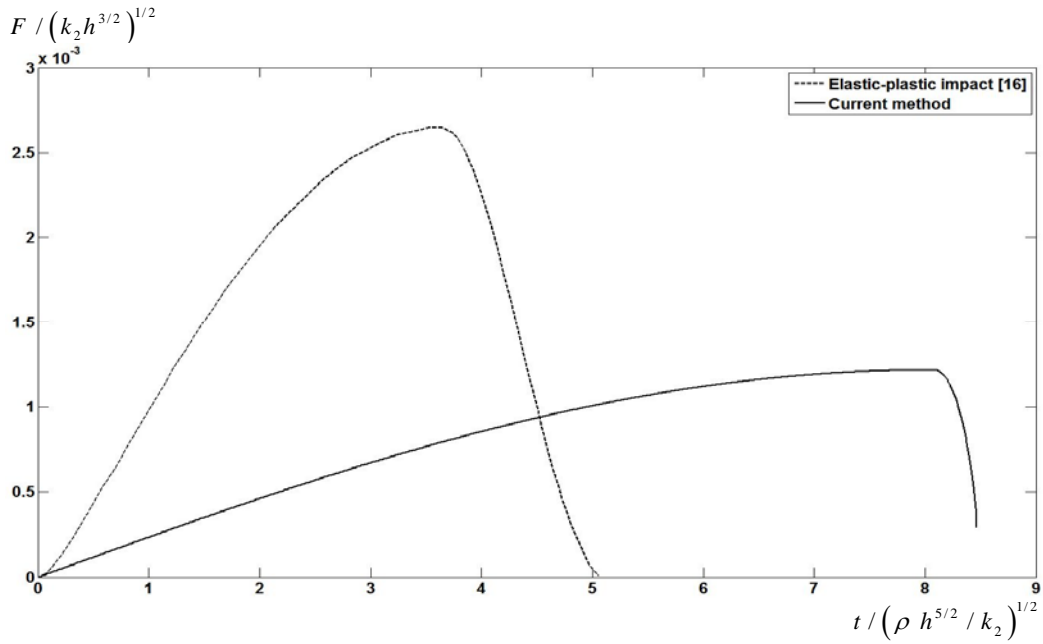
Figure 5 Comparing of impact force history with Ref. [16]

There are many theory of elastic-plastic contact. The theory used in this article is known as Andrew's theory. It is used by several researchers in recent years [24-27]. Variation of the non-dimensional central transverse displacement $\psi_3 E_p a\, h\, /\left(q_0 b^3\right)$ against the dimensionless time $t\sqrt{E\,/\,\rho}\,/b$ for simply supported Mindlin plate are shown in Figs. (6)- (8) using $\upsilon_p = 0.15,\ \ \kappa^2 = \pi^2/12,\ \ \delta = 0.1$ and $\eta = 1$.
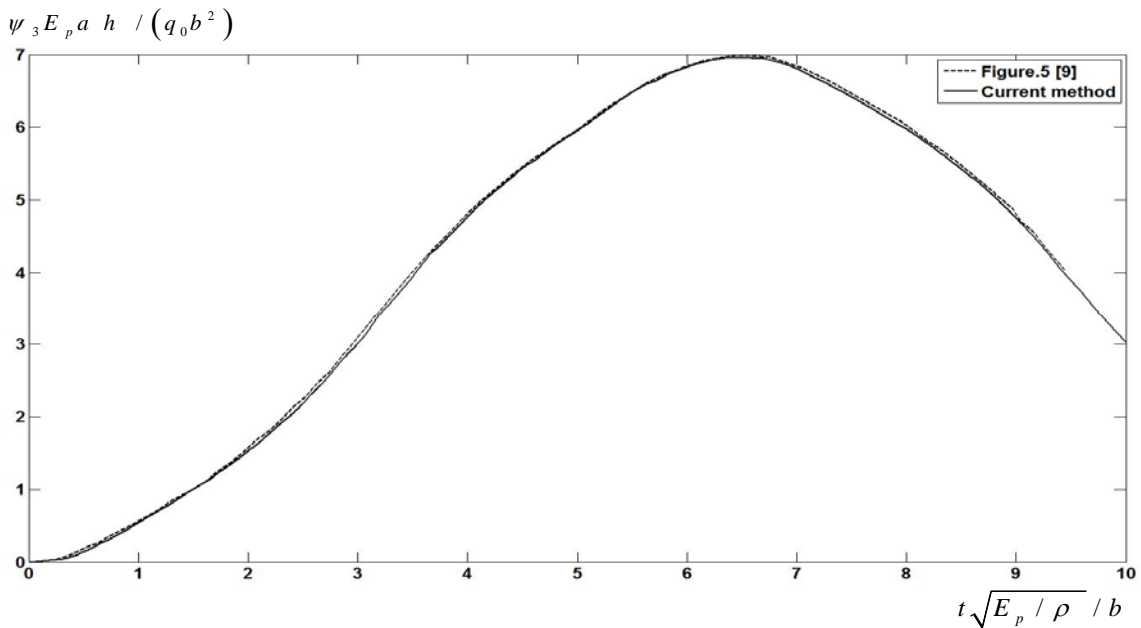
Figure 6 Comparing of non-dimensional central displacement history with Ref. [9]

In Fig. (6) the plate is subjected to in-plane load in the X_1 direction with magnitude $\tilde{N}_1 = -0.25\tilde{N}_{cr}$ and resting on elastic foundation with foundation stiffness parameters $12\upsilon_1\delta^2\eta^4\tilde{K}_1/(\pi^4\lambda) = 2$ and $12\upsilon_1\delta^2\eta^2\tilde{K}_2/(\pi^2\lambda) = 1$, $(\lambda = 0.5)$.

$\psi_3 E_p\, a\; h\;\; /\left(q_0 b^2\right)$
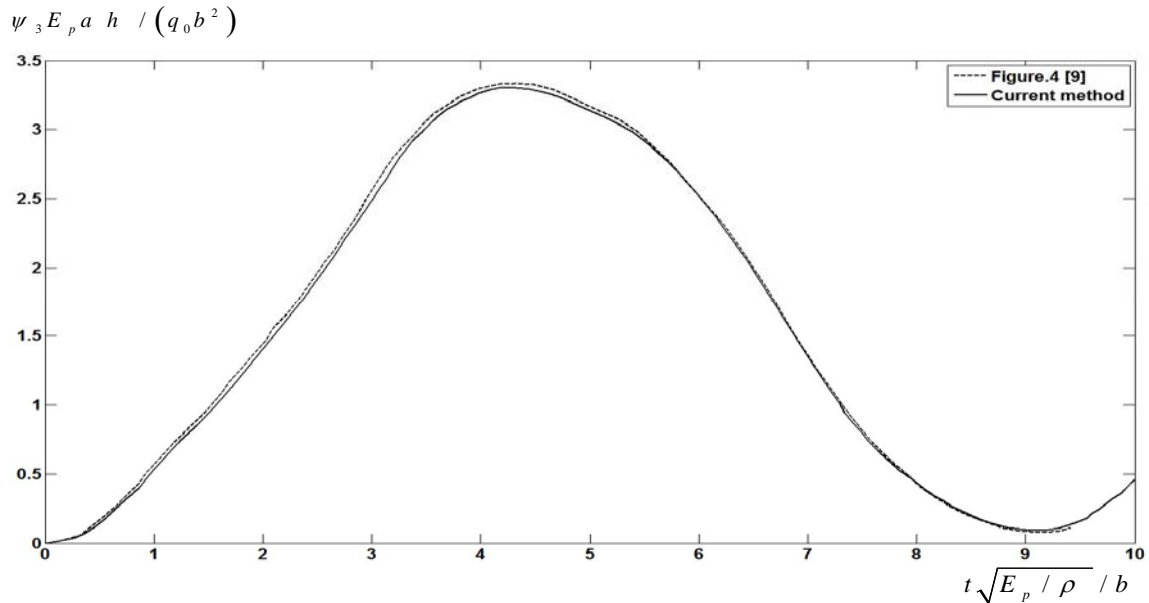
Figure 7 Comparison of the non-dimensional central displacement history with [9]

In Fig. 7 the plate is the same as plate described in Fig. 6 but having no foundation. In Fig. 8 the plate is not subjected to in-plane load but resting on elastic foundation with the same coefficients as described for plate in Fig 6. All three cases are compared with those given in reference [9] and good agreement can be observed.

$\psi_3 E_p a\; h\;\; /\left(q_0 b^2\right)$
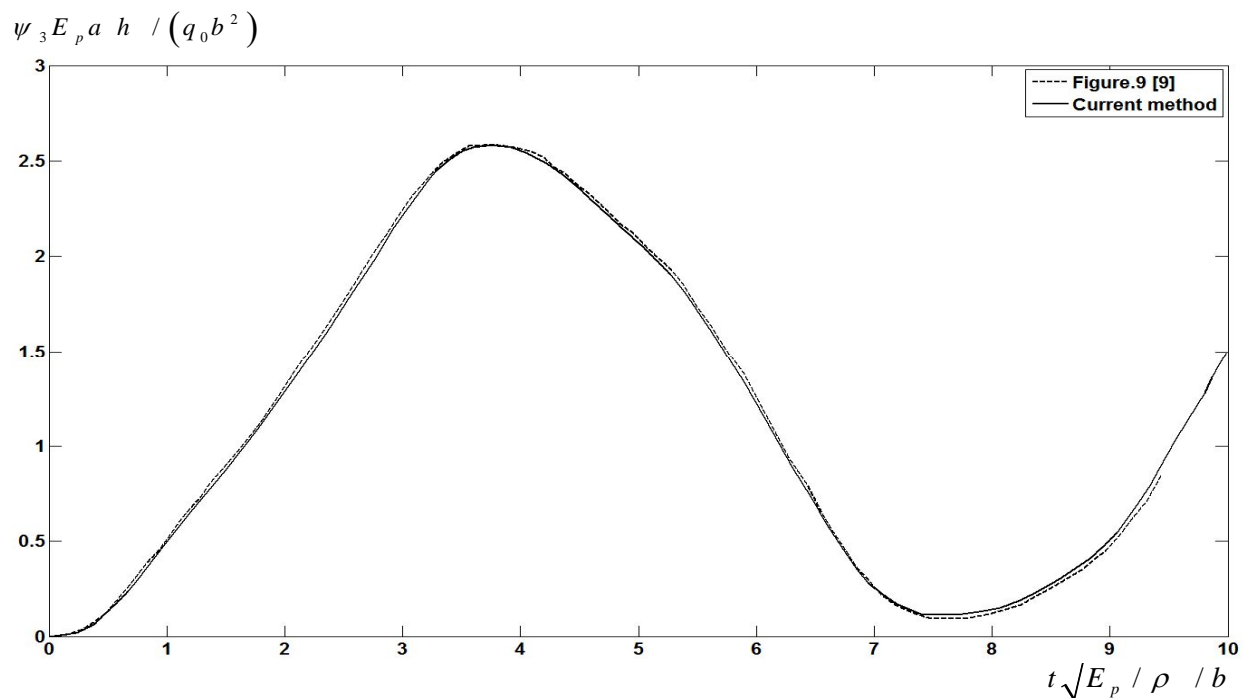
Figure 8 Comparison of the non-dimensional central displacement history with [9]

In order to study the effect of the Winkler stiffness parameter on the force-time history the dimensionless force is plotted against the dimensionless time for a simply supported plate using data given in Table 1 but replacing $\xi = 100$. The result is displayed in Fig. 9. Similar plot is also obtained for the displacement-time history and the result is shown in Fig. 10.
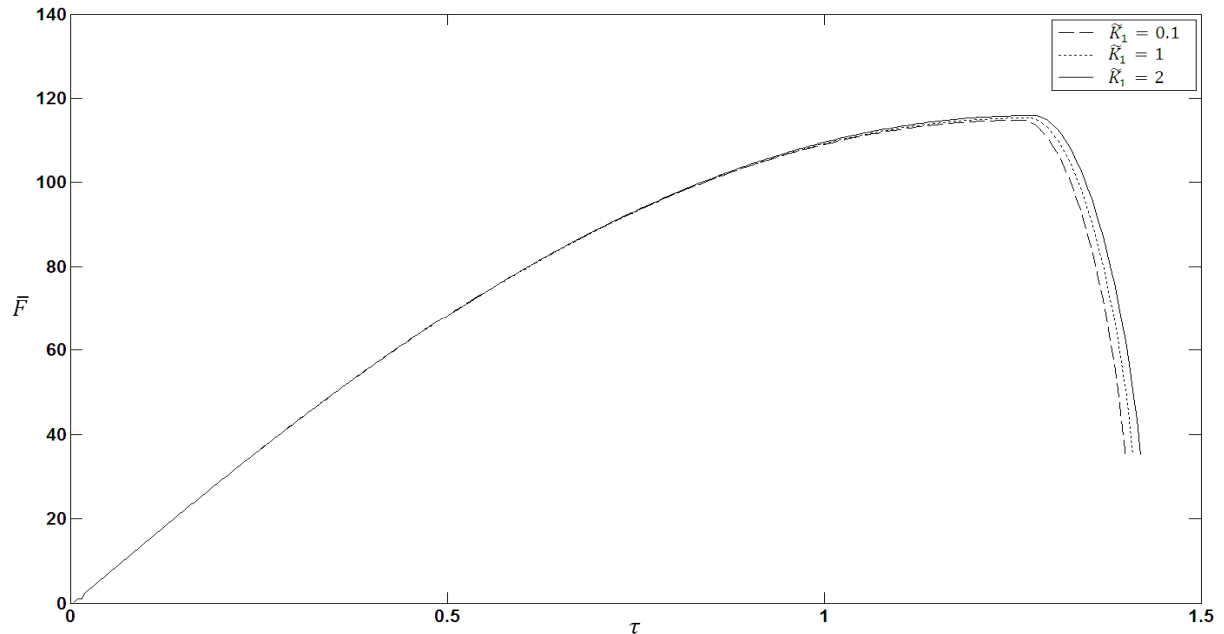

Figure 9 Effect of Winkler stiffness of elastic foundation on impact force history

It can be clearly seen in Fig. 9 that increasing the Winkler stiffness parameter causes a little effect on the impact force, although slight increase can be observed but an increase in duration of contact is more dominant. Reduction in the central displacement of the plate due to increasing the Winkler stiffness parameter may be observed in Fig. 10.
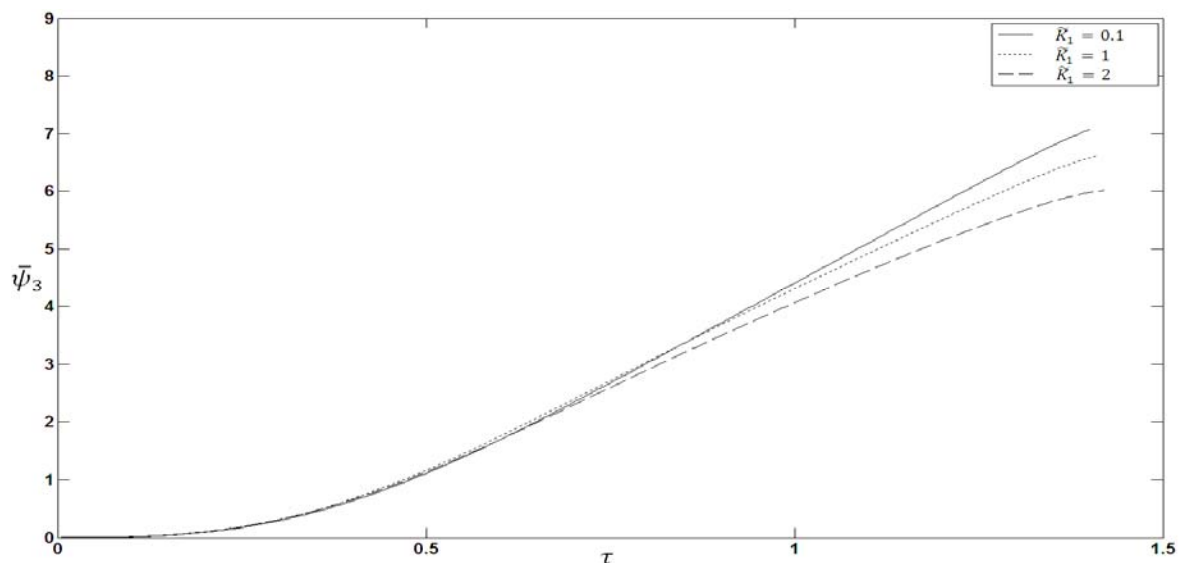
Figure 10 Effect of Winkler stiffness of elastic foundation on displacement history

This is because of increase in resistance of the plate as a result of increasing stiffness. To investigate the effect of shear stiffness parameter similar studies are carried out through Figs. 11 to 14. As shown in these Figs. the same effects as explained for the effects of the Winkler stiffness parameter can be observed on both force-time and displacement-time histories.
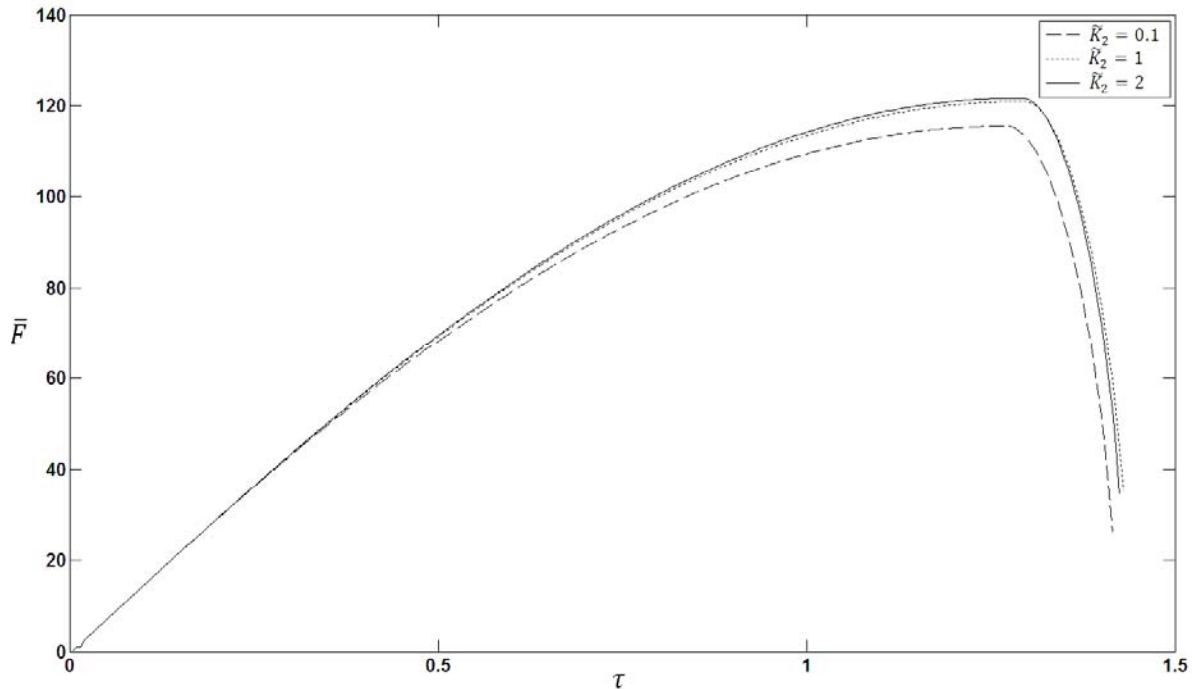

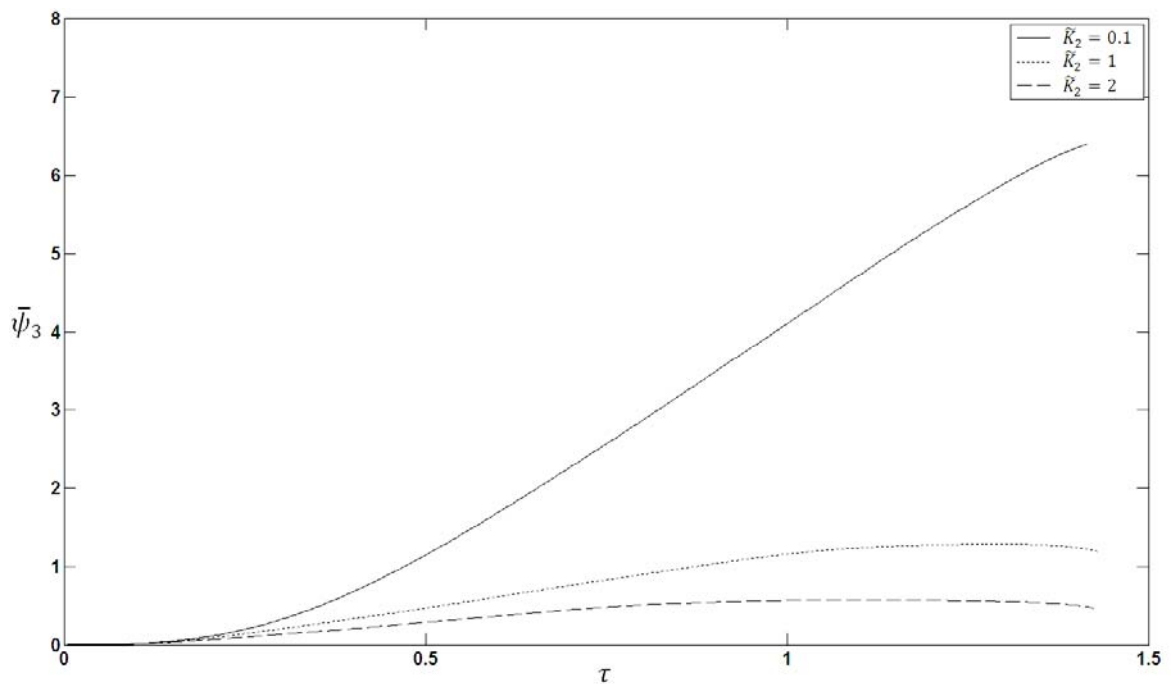**Figure 11** Effect of shear foundation coefficient on impact force history

Figure 12 Effect of shear foundation coefficient on displacement history
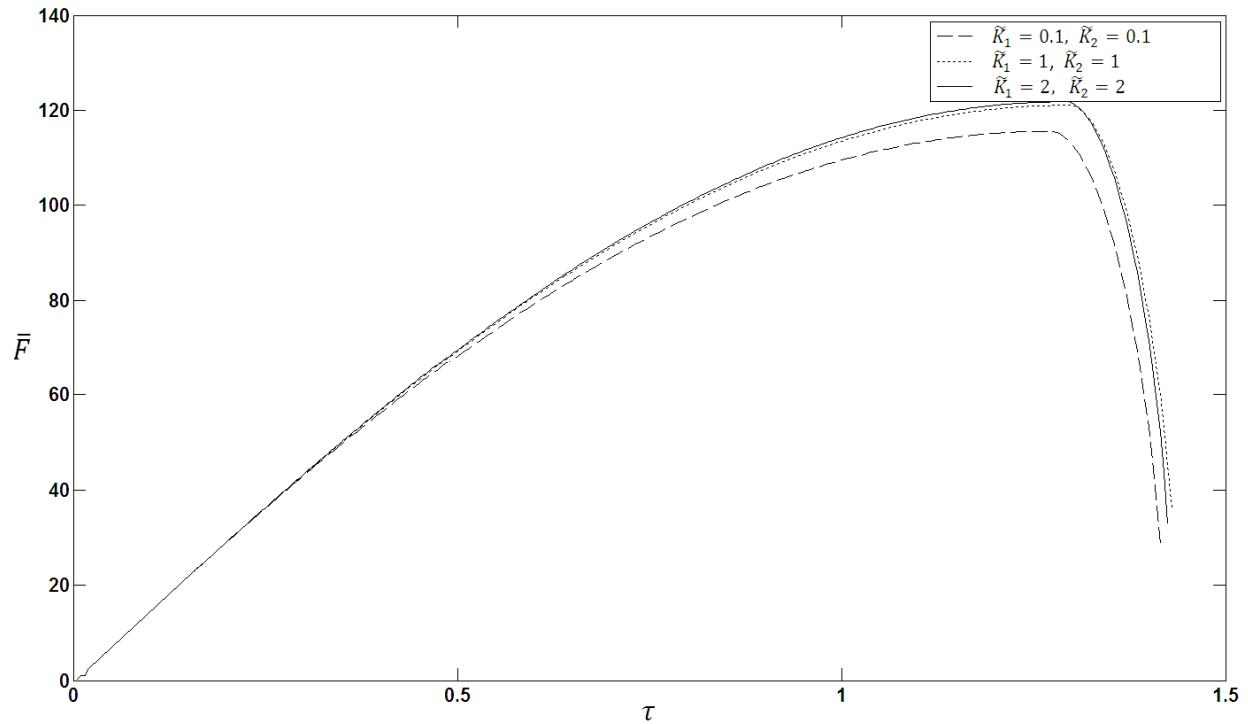
Figure 13 Effects of both elastic foundation stiffness parameters on impact force history

However as far as the effects of Winkler and shear stiffness parameters on the plate response is concern the more dominant effects may be performed by the shear stiffness parameter.
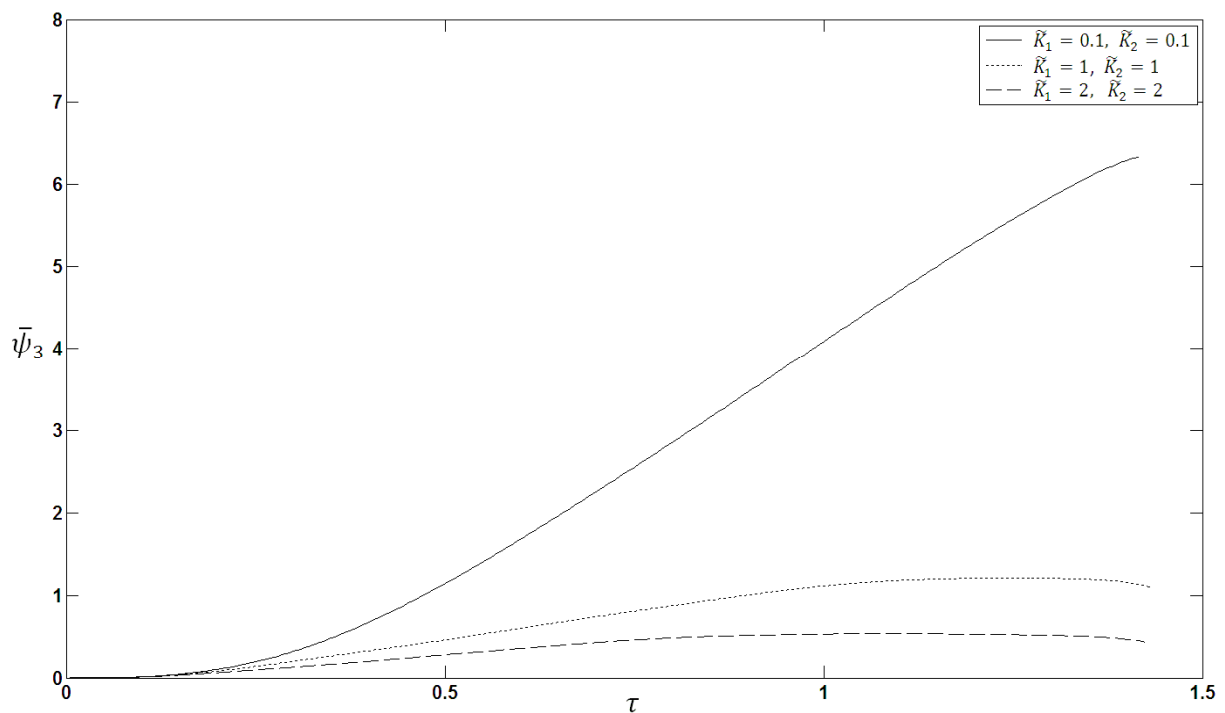

Figure 14 Effects of both elastic foundation stiffness parameters on displacement history

The effect of in-plane load on the force-time history for SCSS plate is investigated in Fig. 15 using data given in Table 1 and selecting new value for ξ as $\xi = 100$.
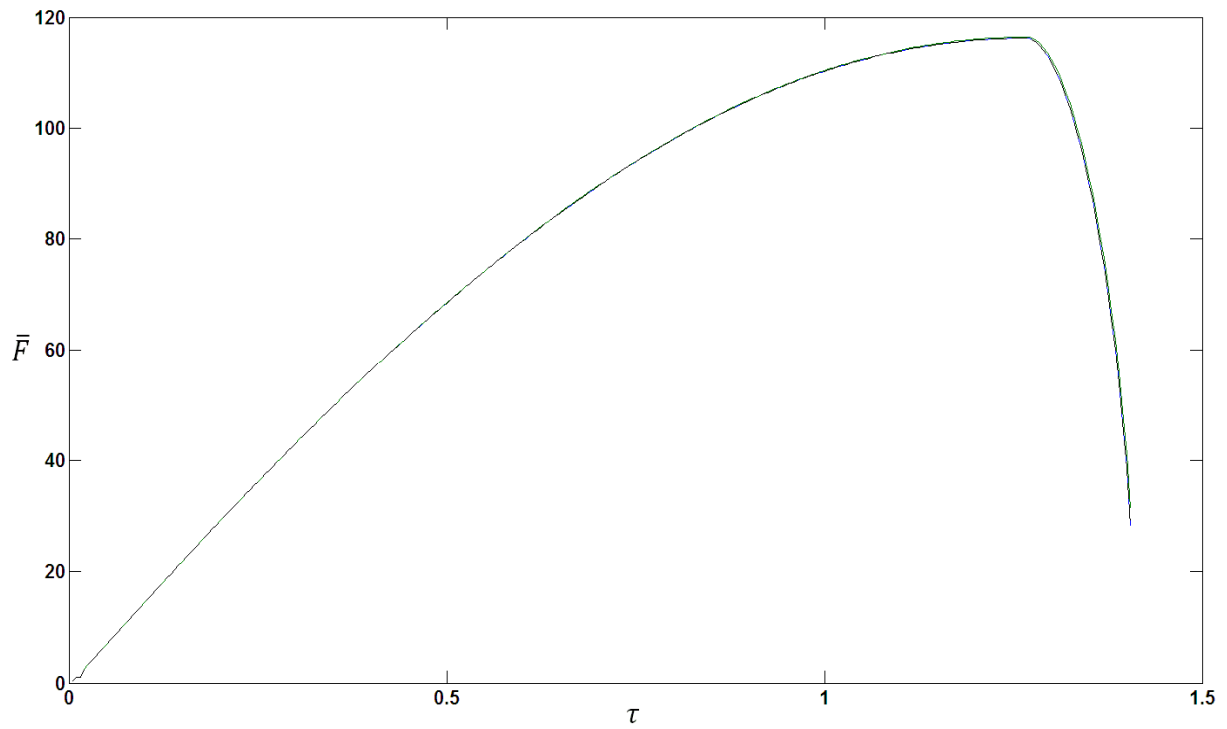
Figure 15 Effect of in-plane load coefficient in X_1 direction on impact force history

It is shown that the variations of the in-plane load have a very little effect on the force-time history. The effect of the in-plane load on the displacement-time history is also displayed in Figs. 16 and 17 for a plate under uniaxial in-plane load in the X_1 direction.
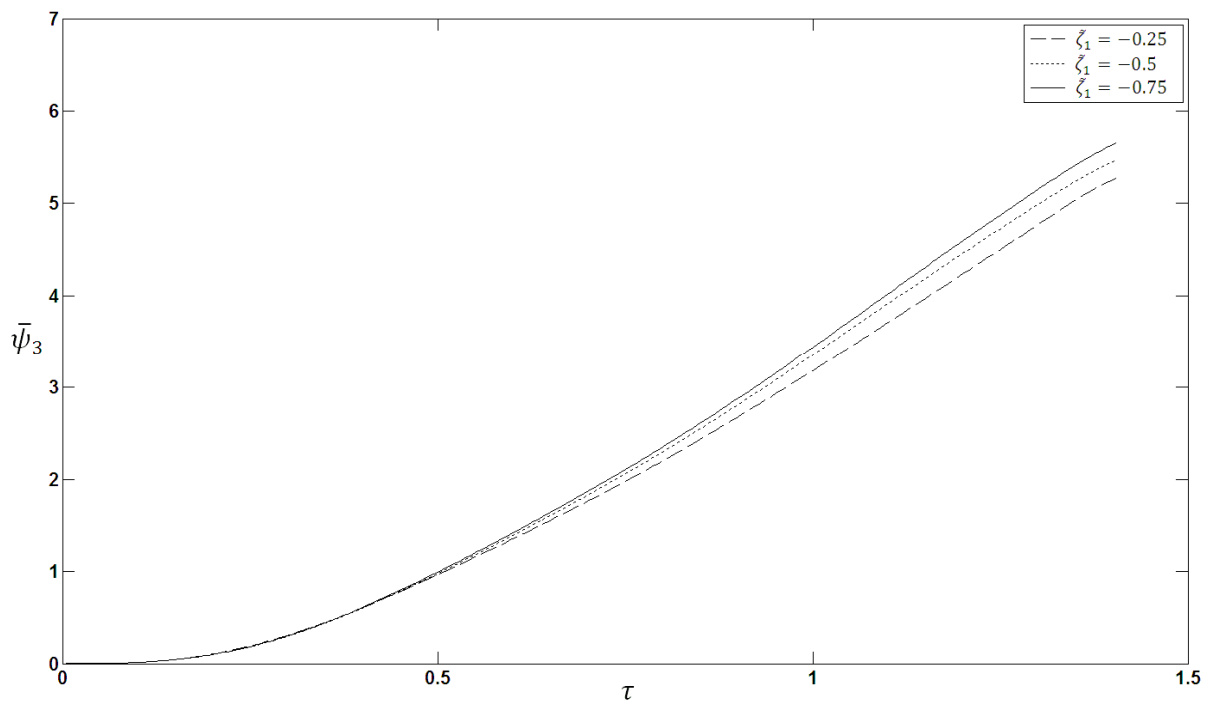

Figure 16 Effect of in-plane load coefficient in X_1 direction on displacement history
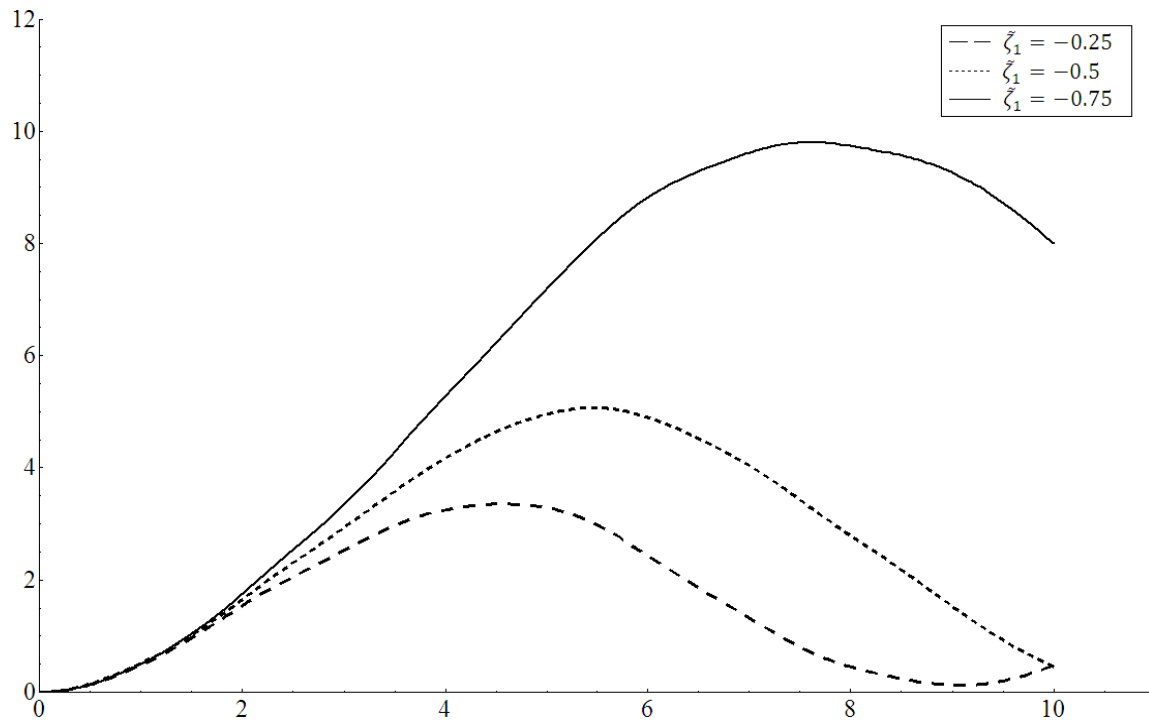
Figure 17 Effect of uniaxial in-plane load acting in the X_1 direction on central displacement-time history of the plate subjected to central impulsive load

It can be observed that as the in-plane load increases the non-dimensional central displacement decreases. The same effect may be seen in Fig. 18 when the plate is subjected to biaxial load in both X_1 and X_2 directions.
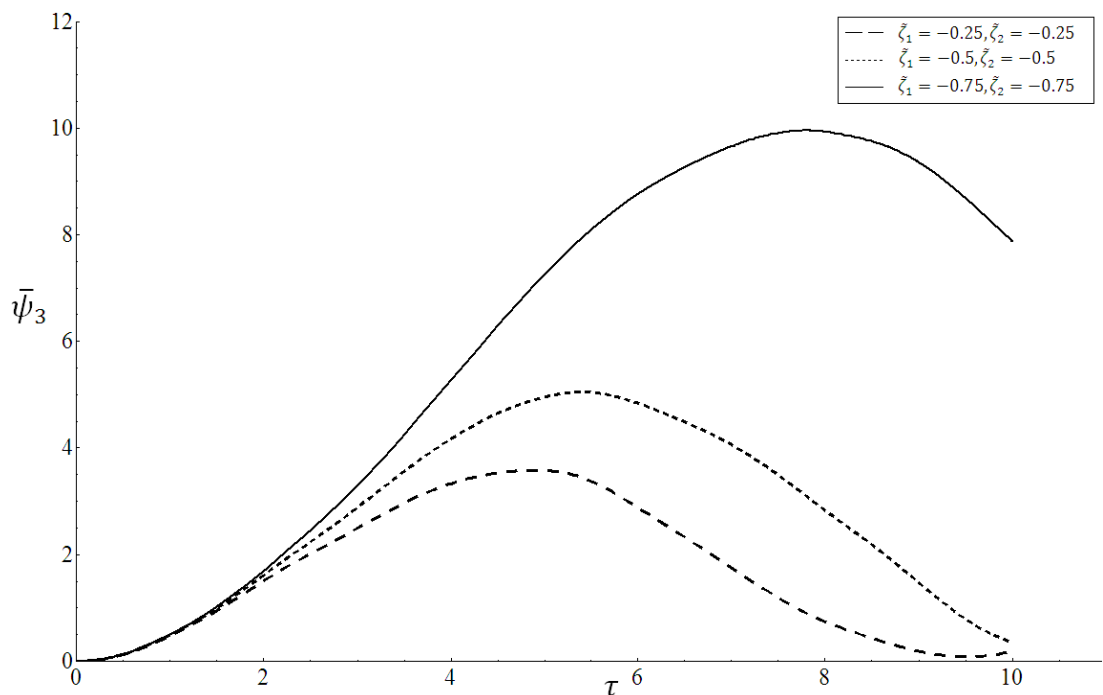

Figure 18 Effect of biaxial in-plane load on non-dimensional central displacement-time history of the plate subjected to central impulsive load

7 Conclusion

The elastic-plastic impact on relatively thick rectangular plate with two opposite edges simply supported and resting on Pasternak elastic foundation is investigated.
 The dimensionless equations of motion are derived based on the Mindlin plate theory considering the in-plane load.
The eigenvalue expansion method is used to obtain the response of the plate to the impulsive load.
The force-time history is calculated by means of small time increment method.
The shear deformation and rotary inertia could effect the force-time history.
As a result of using the closed form solution of eigenvalues and their corresponding mode shape functions, in obtaining the response of the plate to the impulsive load, the present method consumes less calculation time in comparison with the Rayleigh- Ritz method.
The effect of the in-plane load and elastic foundation parameters on the impact force and the displacement histories are investigated and discussed.

Refrences

[1]   Abrate, S., "Impact on Composite Structures," University Press, Cambridge, England (2000).

[2]   Lee, Y. C., and Reismann, H., "Dynamics of Rectangular Plates", International Journal of Engineering Science, Vol. 7, pp. 93-113, (1969).

[3]   Reidmann, H., and Tendorf, Z. A., "Dynamics of Initially Stress Plates," Transaction of the ASME, Journal of Applied Mechanics, Vol. 43, pp. 304-308, (1976).

[4]   Reidmann, H., and Lxu, H.H, "Forced Motion of an Initially Stressed Rectangular Plate –an Elasticity Solution," Journal of Sound and Vibration, Vol. 55, No. 3, pp. 405-418, (1977).

[5]   Sakata, T., and Sakata, Y., "Forced Vibration of a Non-uniform Thickness Rectangular Plates with Two Free Sides," Journal of Sound and Vibration, Vol. 64, No. 4, pp. 573-581, (1979).

[6]   Laura, P.A.A., Avalos, D.R., and Larrondo, H.A., "Forced Vibrations of Simply Supported Anisotropic Rectangular Plates," Journal of Sound and Vibration, Vol. 220, No. 1, pp. 178-185, (1999).

[7]   Shen, H.S., Yang, J., and Zhang, L., "Free and Forced Vibration of Reissner-Mindlin Plates with Free Edges Resting on Elastic Foundation," Journal of Sound and Vibration, Vol. 244, No. 2, pp. 220-320, (2001).

[8]   Yu, L., Shen, H.S., and Huo, X.P., "Dynamic Responses of Reissner-Mindlin Plates with Free Edges Resting on Tensionless Elastic Foundations," Journal of Sound and Vibration, Vol. 299, pp. 212-228, (2007).

[9]   Shen, H.S., Yang, J., and Zhang, L., "Dynamic Response of Reissner-Mindlin Plates under Thermomechanical Loading and Resting on Elastic Foundations," Journal of Sound and Vibration, Vol. 232, No. 2, pp. 309-329, (2000).

[10] Rossikhin, Y.A., and Shitikova, M.V., "Dynamic Response of a Pre-stressed Transversely Isotropic Plate to Impact by an Elastic Rod," Journal of Vibration and Control, Vol. 15, No. 1, pp. 25–51, (2009).

[11] Sun, C. T., and Chattopadhyay, S., "Dynamic Response of Anisotropic Laminated Plates under Initial Stress to Impact of a Mass," ASME Journal of Applied Mechanics, Vol. 42, pp. 693–698, (1975).

[12] Sun, C. T., and Chen, J. K., "On the Impact of Initially Stressed Composite Laminates," Journal of Composite Materials, Vol. 19, pp. 490–504, (1985).

[13] Wei, H., and Yida, Z., "Linear Analysis Method for the Dynamic Response of a Winkler Foundation-supported Elastic Plate Subjected to Low Velocity Projectile Impact," Journal of Vibration and Acoustics, Vol. 116, No. 1, pp. 67-70, (1994).

[14] Nath, Y., and Varma, K., "Nonlinear Dynamic Response of Rectangular Plates on Linear Elastic Foundation," Computers & Structures, Vol. 24, No. 3, pp. 391-399, (1986).

[15] Chattopadhyay. S., "Response of Elastic Plates to Impact Including the Effects of Shear Deformation," In: Recent Advances in Engineering Science (Edited by G. C. Sih). pp. 127-138, Lehigh University Press. Bethlehem, PA (1977).

[16] Chattopadhyay. S., and Saxena, R., "Combined Effects of Shear Deformation and Permanent Indentation on the Impact Response of Elastic Plates," International Journal of Solid Structures, Vol. 27, No. 13, pp. 1739-1745, (1991).

[17] Mittal, R. K., "A Simplified Analysis of the Effect of Transverse Shear on the Response of Elastic Plates to Impact Loading," International Journal of Solids Structures, Vol. 23, No. 8, pp. 1191-1203, (1987).

[18] Ching-Shih, Y., and Enboa, W., "On the Inverse Problem of Rectangular Plates Subjected to Elastic Impact, Part I: Method Development and Numerical Verification," ASME Journal of Applied Mechanics, Vol. 62, No. 3, pp. 692-698, (1995).

[19] Leissa, A.W., and Kang, J.H., "Exact Solutions for Vibration and Buckling of an SS-C-SS-C Rectangular Plate Loaded by Linearly Varying In-plane Stresses," International Journal of Mechanical Sciences, Vol. 44, pp. 1925–1945, (2002).

[20] Kang, J.H., and Leissa A.W., "Vibration and Buckling of SS-F-SS-F Rectangular Plates Loaded by In-plane Moments," International Journal of Stability and Dynamics, Vol. 1, pp.527–543, (2001).

[21] Leissa, A.W., "The Free Vibration of Rectangular Plates," Journal of Sound and Vibration, Vol. 31, pp. 257–293, (1973).

[22] Hosseini-Hashemi, S., Khorshidi, K., and Amabili, M., "Exact Solution for Linear Buckling of Rectangular Mindlin Plates," Journal of Sound and Vibration, Vol. 315, pp. 318–342, (2008).

[23] Christoforou, A.P., and Yigit, A.S., "Transient Response of a Composite Beam Subject to Elastic-plastic Impact," Composites Engineering, Vol. 5, No. 5, pp. 459-470, (1995).

[24] Johnson, K. L., "*Contact Mechanics*," Cambridge University Press, New York (1985).

[25] Olsson, R., "Mass Criterion for Wave Controlled Impact Response of Composite Plates," Composites Part A: Applied Science and Manufacturing, Vol. 31, No. 8, pp. 879–887, (2000).

[26] Chen, L. B., Xi, F., and Yang, J. L., "Elastic–plastic Contact Force History and Response Characteristics of Circular Plate Subjected to Impact by a Projectile," Acta Mech. Sin. Springer-Verlag, Vol. 23, pp. 415–425, (2007).

[27] Pashah, S., Massenzio, M., and Jacquelin, E., "Prediction of Structural Response for Low Velocity Impact," International Journal of Impact Engineering, Vol. 35, pp. 119–132 (2008).

[28] Jacquelin, E., Laine, J.P., Bennani, A., and Massenzio, M., "A Modeling of an Impacted Structure Based on Constraint Modes," Journal of Sound and Vibration, Vol. 301, pp. 789–802, (2007).

Nomenclature

a , b	Length and width of plate
D	Flexural rigidity of plate
E_i	Young's modulus of impactor
E_p	Young's modulus of plate
$F(t)$	Non-dimensional impact force
$\bar{F}(\tau)$	Shear modulus of plate
G	Shear modulus of plate
h	Plate thickness
i	$\sqrt{-1}$
$\tilde{K}_1$	Winkler parameter of elastic foundation
$\tilde{K}_2$	Transverse parameter of elastic foundation
M_{ij}	Resultant moments (i,j=1,2,3)
m_i	Mass of impactor
m_p	Mass of plate
$\tilde{N}_1, \tilde{N}_2$	Non-dimensional in-plane load
$\bar{p}\left(\bar{X}_1, \bar{X}_2, \tau\right)$	Transverse impact of the impactor on plate
Q_k	Transverse shear forces (k=1,2)
R_i	Radius of impactor
q_0	Yield stress
t	Time
V_0	Initial velocity of impactor

W_j	Dimensionless potentials
$X_1 = \overline{X}_1, X_2 = \overline{X}_2$	Cartesian coordinate of position of impact load on plate

Greek symbols

α	Indentation
$\overline{\alpha}$	Non-dimensional indentation
α_1	Elastic indentation in elastic-plastic law
$\alpha_{\max}$	Maximum indentation in elastic law
α_2	Maximum indentation in elastic-plastic law
υ_p	Poisson's ratio of plate
υ_i	Poisson's ratio of impactor
δ	Thickness to length ratio of plate
η	Aspect ratio of plate
ξ	Non-dimensional initial velocity
ρ_i	Mass density of impactor
ρ	Mass density of plate
$\psi_{1,2}$	Rotational displacements
ψ_3	Transverse displacement
$\overline{\psi}_i$	Dimensionless displacement of the impactor
φ	Normalized time parameter
λ	Impact parameter
κ^2	Shear correction factor
τ	Dimensionless time
ω	Natural frequency of plate
β^{mn}	Non-dimensional frequency

چکیده

در این مقاله ضربه الاستوپلاستیک ناشی از برخورد یک کره بر روی یک ورق مستطیلی نسبتا ضخیم که تحت تاثیر نیروهای صفحه ای یکنواخت توزیعی قرار دارد مورد مطالعه قرار گرفته است. ورق بر روی بستر الاستیک پستر ناک مستقر بوده و دارای تکیه گاهای ساده در دو لبه موازی میباشد. دو لبه موازی دیگر ورق میتوانند هرنوع ترکیبی از تکیه گاهای کلاسیک، از قبیل ساده، گیر دار و یا آزاد را شامل شوند. معادلات حاکم بر ارتعاشات آزاد و اجباری بر اساس استفاده از تیوری میندلین با لحاظ نمودن اثرات تغیر شکل برشی و اینرسی چرخشی بشکل بی بعد جهت تسهیل محاسبات و تعمیم نتایج ارایه شده اند. بر اساس تیوری بکار گرفته شده در تحلیل ضربه الاستو پلاستیک مدت زمان دوام تماس شامل سه مرحله است. این مراحل عبارتند ازمرحله فشرده گی الاستیکی اولیه، مرحله فشرده گی بیشتر که در پایان منجر به یک دایره پلاستیک احاطه شده بوسیله یک حلقه الاستیک میشود و بالاخره مرحله بازگشت که در پایان تغیر شکل دایمی را موجب میگردد. نیرو و تقرب در هر یک از مراحل با استفاده از روش نمو کوچک زمانی حل شده است. جهت اعتبار سنجی نتایج بعد از بررسی همگرایی، یافته ها با نتایج ارایه شده توسط سایر محققین مورد مقایسه قرار گرفته و توافق خوبی ملاحظه گردیده است. درپایان اثرات پارامترهای بی بعد از قبیل اثرات نیروهای صفحه ای تک محوری و دو محوری و اثرات پارامترهای سفتی بستر الاستیک در رفتارهای نیرو- زمان و جابجایی- زمان مورد بررسی قرارگرفته اند.